Atmos. Chem. Phys. Discuss., 9, 10675–10710, 2009
www.atmos-chem-phys-discuss.net/9/10675/2009/

Atmospheric Chemistry and Physics Discussions

This discussion paper is/has been under review for the journal *Atmospheric Chemistry and Physics (ACP)*. Please refer to the corresponding final paper in *ACP* if available.

Decadal regional air quality simulations over Europe in present climate: near surface ozone sensitivity to external meteorological forcing

E. Katragkou[1], P. Zanis[2], I. Tegoulias[2], D. Melas[1], B. C. Krüger[3], P. Huszar[4], T. Halenka[4], and S. Rauscher[5]

[1]Laboratory of Atmospheric Physics, Aristotle University of Thessaloniki, Greece
[2]Department of Meteorology and Climatology, Aristotle University of Thessaloniki, Greece
[3]Inst. of Meteorology, Univ. of Natural Resources and Applied Life Sciences, Vienna, Austria
[4]Dept. of Meteorology and Environment Protection, Charles University, Prague, Czech Republic
[5]Earth System Physics Section, The Abdus Salam International Centre for Theoretical Physics (ICTP), Trieste, Italy

Received: 14 April 2009 – Accepted: 22 April 2009 – Published: 4 May 2009

Correspondence to: E. Katragkou (katragou@auth.gr)

Published by Copernicus Publications on behalf of the European Geosciences Union.

Abstract

Regional air quality decadal simulations were carried out using the air quality model CAMx driven off-line by the regional climate model RegCM3 for the time slice 1991–2000 using two different datasets of external meteorological forcing to constrain RegCM3: the ERA40 global atmospheric reanalysis dataset and the output from the GCM ECHAM5. The focus of this work is to compare the perfect lateral boundary conditions experiment with the GCM driven control experiment and to investigate how this external meteorological forcing affects near surface ozone. The different RegCM3 meteorological forcings resulted in changes of near surface ozone over Europe ranging between ±5 ppb for winter and summer, while all model parameterizations and anthropogenic emissions remained unchanged. Changes in near surface ozone are induced by changes in meteorological fields and biogenic emissions, which are on-line calculated and meteorology-dependent. The model simulations suggest that the change in solar radiation is the factor that mostly modulates the ozone changes in summer. During winter season it is found that the induced changes in NO_x explain about 40% of the ozone variability. The meteorological induced changes in biogenic emissions are quite low for winter with rather small impact on ozone while they are more temperature than radiation dependent. Using multiple regression analysis to associate the changes in near surface ozone with the respective changes in selected meteorological parameters and ozone precursors, an explained variance of 70% in summer and 60% in winter is reproduced.

1 Introduction

Tropospheric ozone is an important trace gas controlling the oxidation capacity of the atmosphere with well documented adverse effects on human health (Schlink et al., 2006), agriculture (Fuhrer et al., 2003) and natural ecosystems (Scebba et al., 2006). Tropospheric ozone chemistry includes a large set of complex photochemical reactions

ACPD

9, 10675–10710, 2009

involving NO_x (=NO_2+NO) and volatile organic compounds (VOCs) (Crutzen, 1988; Penket, 1988; Seinfeld and Pandis, 1998). Ozone precursors have natural as well as anthropogenic sources, the most important of which are emissions from soil/vegetation and fossil fuel combustion. Ambient ozone concentrations depend strongly on availability and relative abundance of those gaseous precursors but they are also modulated by the meteorological conditions (Davies et al., 1992; Kalabokas et al., 2008).

Global change including change in climate and anthropogenic emissions of O_3 precursors is expected in the 21st century (IPCC, 2007). Understanding the way that air quality is affected by changes in climate and emissions is of major importance. The direction of change is not always clear because of multiple competing effects. There have been numerous studies on the impact of individual meteorological parameters on ozone concentrations. The parameters that are mostly found to affect ozone concentrations are temperature, solar radiation, water vapor concentration, mixing height, wind, cloud liquid water path and precipitation (Bloomfield et al., 1996; Davis et al., 1998; Sillman and Samson, 1995; Khalid and Samson, 1996; Broennimann and Neu, 1997; Baertsch-Ritter et al., 2004; Dawson et al., 2007). These parameters are not independent with each other and may have multiple effects on ozone production. Temperature, for example, alters chemical reaction rates that control the ozone budget, change PAN production, thereby affecting the NO_x balance and thus ozone production and control temperature-sensitive biogenic emissions which are known to impact strongly ozone production (Fiore et al., 2005). Solar radiation also impacts on biogenic emissions directly and indirectly through temperature, since solar radiation and temperature are closely related. It is therefore a complex issue to unravel the effects of different meteorological parameters on air quality in real atmosphere because of the interdependence and the multiple feedbacks.

A more holistic approach is to study the impact of climate change on air quality which is a far more complicated task involving climate change, feedbacks with climate-dependent biogenic emissions and changes in future anthropogenic emission trends. Most of the studies investigating the future air quality projections were based on global

Climate-Chemistry models or global climate models coupled to chemistry-transport models (Hauglustaine et al., 2005; Stevenson et al., 2006; Racherla and Adams, 2006; Hedegaard et al., 2008; Racherla and Adams, 2008, and references therein) and only few studies give emphasis on the regional scale future air-quality (Szopa et al., 2006; Meleux et al., 2007; Nolte et al., 2008).

This paper presents a modeling system based on the air quality model CAMx driven off-line by the regional climate model RegCM3 for the assessment of regional air quality over Europe on decadal timescale with focus on the sensitivity of near surface ozone on the lateral meteorological boundary conditions constraining RegCM3. Validation of the modeling system against measurements is described in detail elsewhere (Tegoulias et al., 2009). The wider scope of this work is to investigate the credibility of our modeling system which is driven by the ECHAM5 general circulation model (GCM) in order to further use it for future scenarios including climate change. This task is accomplished by performing a decadal climate-air quality run twice, once driven by the GCM ECHAM5 (GCM driven control experiment) and then by the ERA40 reanalysis (perfect lateral boundary conditions experiment), which serves as the reference.

2 Description of the modeling system

The modeling system applied to simulate regional air quality over Europe in decadal time slices is RegCM3/CAMx. The RegCM3/CAMx modeling system is based on the air quality model CAMx driven off-line by the regional climate model RegCM3 (RegCM version 3). The regional climate model RegCM version 3 (Pal et al., 2007) used for the regional climate simulations in this study, was originally developed at the National Center for Atmospheric Research (NCAR) and has been mostly applied to studies of regional climate and seasonal predictability around the world (Giorgi et al., 2006; Pal et al., 2007). The dynamical core is based on the hydrostatic version of the NCAR-PSU Mesoscale Model version 5 (MM5) (Grell et al., 1994). The radiative transfer package is taken from the Community Climate Model version 3 (CCM3) (Kiehl et al., 1996).

ACPD
9, 10675–10710, 2009

The large-scale cloud and precipitation computations are performed by Subgrid Explicit Moisture Scheme (SUBEX; Pal et al., 2000). Ocean surface fluxes are computed according to the scheme of Zeng et al. (1998) and the land surface physics according to Biosphere-Atmosphere Transfer Scheme (BATS; Dickinson et al., 1993). The adopted convective scheme for the RCM simulations in this study is the Grell scheme (Grell, 1993) with the Fritsch and Chappell (1980) closure assumption. RegCM3 was used to simulate the time period 1960–2002 for a large European domain with a grid resolution of 50 km×50 km. This long-term simulation of RegCM3 was carried out at ICTP (International Centre for Theoretical Physics) within the framework of the EU project ENSEMBLES.

The air quality model simulations were performed with the Comprehensive air quality model with extensions (CAMx) version 4.40 developed by ENVIRON (http://www.camx.com). CAMx is off-line coupled to RegCM3 with a FORTRAN-based code interface, which reads the basic meteorological parameters from RegCM3 and converts them into format accepted by CAMx. Fields required by CAMx but not available directly in the RegCM3 output are calculated within this interface using diagnostic procedures. Pressure and geopotential height is obtained using the hydrostatic formula, the vertical profile of temperature and humidity and the precipitation rates are used to compute the cloud/rain water content and cloud optical depth and, finally, the vertical diffusion coefficients are calculated following O'Brien (1970).

The projection of both models is identical (Lambert Conformal Conic) in order to avoid interpolations between grids that usually introduce large errors. The spatial resolution of CAMx therefore was set to 50 km×50 km. The domain's vertical profile contains 12 layers of varying thickness. Layer 1 is 36 m deep and the uppermost layer is 1.2 km thick and extends to about 6.5 km. Top and lateral boundary conditions were kept constant corresponding to a clean atmosphere. The chemistry mechanism invoked is Carbon Bond version 4 (CB4). This mechanism includes 117 reactions – 11 of which are photolytic – and up to 67 species (37 gasses, 12 radicals and up to 18 particulates). Both model runs covered the period 1990–2000, however we analyze

the decade 1991–2000 as we consider the first year as spin up time.

Organic biogenic emissions were calculated with the use of the RegCM3-CAMx interface, which extracts meteorological parameters from RegCM3 (temperature and radiation) and uses the available land use categories to calculate emission potentials and foliar biomass densities (Guenther et al., 1993). Anthropogenic emissions were calculated with data from the UNECE/EMEP data base (http://webdab.emep.int/) for European emissions (Vestreng et al., 2005) for the year 2000. These data comprise the annual sums of the emissions of NO_x, CO, non-methane hydrocarbons, SO_2, NH_3, fine particles (<2.5 µm) and coarse particles (2.5 µm to 10 µm) on a 50 km×50 km grid. Eleven sectors of anthropogenic activity are distinguished in accordance to SNAP97. For every sector different distributions for the month, the day of the week and the hour of the day were applied for the temporal disaggregation. The disaggregation factors are taken from the inventory by Winiwarter and Zueger (1996).

Part of the work presented here is accomplished in the framework of the European Project CECILIA (Central and Eastern Europe Climate Change Impact and Vulnerability Assessment). A total of four decadal climate-air quality simulations were performed for this project for the time slices 1991–2000, 2041–2050 and 2091–2100. RegCM3 was forced by the ECHAM5 global circulation model (GCM) for the simulations covering the three different time-slices with the ECHAM5 run under the IPCC A1B scenario to provide forcing for the future decades. The present decade (1991–2000) was simulated twice: by ECHAM5 as a GCM driven control experiment and by ERA40 reanalysis as a perfect lateral boundary conditions experiment. These two runs will be referred to hereafter as ECHAM and ERA runs, respectively. Since the ERA40 reanalysis project is a global atmospheric analysis of observations and satellite data streams it can be considered to be the one closer to real atmospheric conditions and thus is used as the reference run. In this work the latter is compared to the ECHAM run performed for the same decade. The aim of this work is to investigate the suitability of our modeling system forced by the GCM ECHAM to simulate future climate by comparing one decade with a reference run (ERA run). The ERA run was additionally validated for

ACPD
9, 10675–10710, 2009

surface ozone using observation from the EMEP dataset and the results are presented in another paper (Tegoulias et al., 2009). According to Tegoulias et al. (2009) the ERA run yielded near surface ozone concentrations that are well comparable to measurements. Specifically the fractional gross error ranged between 10% and 35% while the mean normalized bias was ±20% in the majority of EMEP stations. Satisfactory model performance is usually considered within the ranges of ±15–20% for normalized bias and 30–35% for gross error according to US-EPA regulations.

In this work the differences between the ERA and the ECHAM run for the decade 1991–2000 are presented. Emphasis is given on how the different meteorological forcing affects near surface ozone, which are the dominating factors and what is their relevant importance for the winter and summer season.

3 Results

3.1 Ozone and NO_x differences

Based on the ERA run, which is the decadal simulation closer to real atmospheric conditions, Fig. 1 shows the average winter and summer near surface ozone concentrations over Europe during the period 1991–2000. Summer ozone is averaged over the months June, July and August and winter ozone from December to February. Some distinct spatial patterns appear in both seasons: Ozone concentrations are lower over the land than over the sea because on the one hand O_3 deposition rates are greater over land than over the sea while on the other hand ozone destruction due to reaction with anthropogenic NO dominates over the continent where the anthropogenic emissions of NO_x are congregated. Besides, due to intense photochemistry in Southern Europe, model calculations yield the highest O_3 concentrations over the Mediterranean basin, attaining values of around 60 ppbv in summer and around 40 ppbv in winter. Over continental Europe the summer values range between 30 and 45 ppb and the winter values around 15–25 ppb. Ozone spatial patterns can be more thoroughly

ACPD
9, 10675–10710, 2009

interpreted if they are examined in association with the respective average NO_x concentration fields (Fig. 2). The highest NO_x concentrations over Europe appear in the proximity of large urban agglomerations with intense industrial activity and dense population, where O_3 exhibits its minimum values. NO_x concentrations are in general higher during winter months obviously reflecting, a) corresponding emission temporal profiles, with increased NO_x emissions during colder months b) the longer chemical lifetime of NO_x during the cold months and c) lower boundary layer heights leading to less dilution of the emissions. Local NO_x monthly maxima in December over UK and Northern Europe are estimated to be around 50 ppb but not higher than 25 ppb in summer.

The Figs. 3 and 4 illustrate the average winter and summer differences between the ECHAM and ERA runs in near surface O_3 and NO_x over Europe. In winter season the average O_3 forced from ECHAM is higher than in ERA run by about 2 to 5 ppbv for a large part of Europe with the highest positive differences seen over Central-eastern and South-Eastern Europe while negative ozone differences are seen over UK, Scandinavia and North Atlantic ocean (Fig. 3a). This pattern of positive/negative ECHAM-ERA O_3 differences is associated with an anti-correlated pattern of negative/positive ECHAM-ERA NO_x differences (Fig. 4a). The correlation coefficient between $\Delta(O_3)$ and $\Delta(NO_x)$ over the whole domain in winter is −0.63 (Table 1a). This anti-correlation indicates that part of the ozone increase/decrease in the ECHAM run is associated with NO_x decrease/increase and hence reduced/increased NO titration by O_3. In summer season the average O_3 forced from ECHAM is lower than in ERA run by a few ppbv for almost the whole model domain except in Eastern Mediterranean, Middle East and Gibraltar (Fig. 3b). The respective NO_x changes in summer are small and mainly seen over Germany and Poland. This indicates that the NO titration effect by O_3 plays only a minor role in summer. Nevertheless the correlation coefficient between $\Delta(O_3)$ and $\Delta(NO_x)$ over the whole domain in summer is still negative being −0.48 (Table 1b).

In a corresponding way to Figs. 3 and 4, Figs. 5–10 show ECHAM minus ERA differences in incoming solar radiation Δ(SR) and cloud liquid water path Δ(CLWP), 500 hPa geopotential height Δ(GH) and surface temperature Δ(T), zonal Δ(U) and meridional

ACPD
9, 10675–10710, 2009

wind component Δ(V) and biogenic emissions Δ(BE). Changes in O_3 concentrations are driven by changes in meteorological fields, caused by the different forcing (ECHAM5 vs. ERA40) – which at the same time affect the dynamics of the atmosphere, biogenic emissions and chemistry.

The response of ozone to a different meteorological forcing is clear and in the following discussion we will try to identify the relative importance of several parameters that control ozone concentrations. Obviously, it is not easy to isolate the role of each parameter that contributes to a change in O_3 fields, since they all interact in a complex way. Multiple step regression analysis is encountered to explain a great part of ozone variance and understand the basic mechanisms that modulate the simulated ozone levels during the summer and winter period.

3.2 Temperature differences

It has been shown in several studies that temperature is a meteorological factor that greatly affects ozone in different ways. Firstly, rate constants involved in ozone chemistry are temperature dependent and secondly, biogenic emissions, which are known ozone precursors, are also temperature dependent. Furthermore changes in air temperature are closely related to atmospheric circulation changes, which in turn influence tropospheric ozone changes in synoptic scale (Davies et al., 1992; Kalabokas et al., 2008). In the modeling study of Dawson et al. (2007), which investigated the impact of several meteorological parameters on ozone, it was shown that of all parameters, the one having the largest impact on ozone was temperature. Ozone exceedances and average daily maximum 8 h concentrations increased almost linearly with temperature. PAN chemistry was found to be largely responsible for the dependence of ozone formation on temperature. Meleux et al. (2007) in their study of summer European ozone reported that temperature driven increase in biogenic emissions appeared to enhance ozone production and isoprene was identified to be the most important chemical factor in the ozone sensitivity. The same conclusion was reached by Hedegaard et al. (2008) with their modeling study of climate change on air pollution, suggesting that

ACPD
9, 10675–10710, 2009

dominating impacts on a large number of species including ozone are related to temperature increase. Figure 5 shows differences in near surface air temperature between the ECHAM and ERA run during winter. Fields of $\Delta(O_3)$ bare some similarities to $\Delta(T)$: ECHAM runs yielded higher temperatures over Europe mainland up to 4 degrees and higher ozone concentrations with similar spatial pattern up to 4 ppb. Mind that the highest positive temperature differences seen over Central-eastern and South-Eastern Europe collocate with the highest positive ozone differences. Similar temperature-ozone spatial patterns with the same sign are also observed over Asia minor and N. Africa, UK and part of the Scandinavian peninsula. In contrast, the increase of temperature of about 2–3 K over the north-west corner of the domain does not appear to be followed by an ozone increase.

The pattern of temperature changes between ECHAM and ERA is quite different in summer. The field of $\Delta(T)$ is mostly negative with the exception of north- and south-west and south-east corners of the domain. Interestingly the more intense decrease of temperature over central Mediterranean can be also observed in O_3 summer average field. On the contrary, the stronger decrease of O_3 in summer over central Europe does not seem to be explained by temperature changes. Overall, the correlation coefficient between $\Delta(O_3)$ and $\Delta(T)$ over the whole domain is 0.26 in winter and 0.36 in summer (Tables 1a and 1b).

3.3 Solar radiation and cloud liquid water path differences

Solar radiation is naturally expected to strongly affect ozone since it controls all photochemical reactions which are involved in ozone production and destruction processes. According to Krüger et al. (2008) increase of net radiation together with temperature are expected to increase ozone concentrations by the end of the century. Comparison of Figs. 3 and 6 which show $\Delta(O_3)$ and $\Delta(SR)$, respectively shows that the correlation between solar radiation and surface ozone is clearly better in summer season than in winter season. Calculation of the correlation coefficient between the two fields yields a relatively good correlation of 0.58 in summer but much lower correlation (0.16) in

ACPD
9, 10675–10710, 2009

winter (Tables 1a and 1b). The main ozone decrease of surface ozone in the ECHAM run in central Europe (around 4–5 ppb) seems to be related to the decrease of solar radiation. The relation of the two fields is easily understood since ozone production is photochemically driven and thus sun-light dependent.

Average plots of the difference ECHAM-ERA in cloud liquid water path (CLWP) are shown in Fig. 7. These plots can be used as an indication of change in cloudiness. As it is expected there is a good agreement between the CLWP and SR fields. Increase of CLPW is accompanied by a decrease in solar radiation. In Table 1 it is shown that there is a significant anti-correlation between CLWP and SR, which ranges from −0.66 in winter to −0.73 in summer. Specifically, in summer, the decrease of solar radiation in the ECHAM run in comparison to ERA is a result of increased cloudiness over Europe in a latitude belt extending from 45° to 65° (Fig. 7). Furthermore, the dipole pattern of SR increase in Eastern Mediterranean and SR decrease over the Iberian Peninsula and adjacent Atlantic Ocean in winter is associated with an anti-correlated dipole pattern in CLPW differences. These differences in cloudiness indicate differences in atmospheric circulation over Europe between ECHAM and ERA simulations and they are discussed more extensively below.

3.4 Geopotential height and wind differences

It is known that atmospheric circulation exerts important influence on the distribution of ozone and its precursors on various scales. Hegarty et al. (2007) showed that certain circulation patterns over northeastern United States, identified with a correlation-based synoptic categorization technique, controlled summertime surface ozone. The 500 mb geopotential height as well as the zonal and meridional wind components are used as indicators for identifying the synoptic scale circulation differences between ECHAM and ERA simulations (Figs. 8 and 9).

The average 1991–2000 winter ECHAM circulation pattern has a more steep geopotential height gradient along Europe, being more anticyclonic over Eastern Europe and more cyclonic over West Europe–East Atlantic. The more anticyclonic conditions over

ACPD
9, 10675–10710, 2009

Eastern Europe are expected to be accompanied with fairer weather conditions, higher temperature, lower cloudiness and higher surface solar radiation levels. These geopotential height differences in winter (Fig. 8) are associated to a certain extend with the respective differences in air temperature (Fig. 5), solar radiation (Fig. 6) and cloudiness (Fig. 7). All these parameters support the build up of high ozone concentrations as well as its photochemical production. Indeed, ozone concentrations are higher in winter over Eastern Europe and decrease over Eastern Atlantic where geopotential heights are lower, probably related to more cyclonic conditions.

The pattern of the geopotential height differences in winter is supported by the respective pattern of differences in zonal and meridional wind components (Fig. 9). Westerlies over the Iberian Peninsula become stronger in ECHAM than in ERA simulations and weaker over northern UK and North Atlantic Ocean while the meridional wind component is characterized by an increased southern zonal flow in ECHAM with its maximum over Germany and Poland. These induced wind changes are expected as a result of the more cyclonic conditions over West Europe–East Atlantic and the more anticyclonic conditions over Eastern Europe.

The field of the 500 hPa GH differences between ECHAM and ERA simulations in summer shows a low over Russia of about −50 m. This feature implies a more cyclonic behavior of ECHAM in the region between 50–55° latitude and 25–40° longitude which is expected to be accompanied with typical cyclonic patterns, i.e. lower temperatures, increased cloudiness and reduced solar radiation. These features are indeed encountered in Δ(T) (Fig. 5), Δ(SR) (Fig. 6) and Δ(CLWP) fields. The correlation coefficient between $\Delta(O_3)$ and Δ(GH) is 0.57 in summer suggesting that atmospheric circulation impacts on surface ozone concentrations, either directly through atmospheric circulation or indirectly through photochemistry. The average difference map of wind components for the summer period shows enhanced westerly winds in mid-latitudes for the ECHAM run (Fig. 9) related to higher West-East GH gradient. A stronger north meridional component is also apparent mainly over Scandinavia (Fig. 9), which is associated with the low seen over Russia in the map of ΔGH.

ACPD
9, 10675–10710, 2009

It is not easy to separate the impact of changing wind fields on surface ozone concentrations. Obviously the wind components agree well with the synoptic circulation features as seen through the Δ(GH) fields. The system is however too interactive to separate the impact of each meteorological parameter on ozone, especially on a decadal scale.

3.5 Differences in biogenic emissions

Biogenic emissions (BE) are known to have a strong impact on surface ozone concentration. The most important biogenic hydrocarbon in atmospheric chemistry is isoprene (C_5H_8) (Seinfeld and Pandis, 1998). The relative magnitudes of isoprene and NO_x emissions determine the impact on O_3 (Fiore et al., 2004). Isoprene oxidation is a large source of hydroperoxy (HO_2) and organic peroxy radicals (RO_2), which can react with NO_x to stimulate O_3 production. In rural areas, especially where NO_x is low, however, O_3 production is considered as NO_x-sensitive and insensitive to VOCs. Under low NO_x emissions, high isoprene emissions can even decrease O_3 by either sequestering NO_x as isoprene nitrates, thereby suppressing O_3 formation or by ozonolysis of isoprene. The treatment of isoprene chemistry by chemical mechanisms of global and regional models has still great uncertainties and their impact on O_3 budget is large. The study of von Kuhlmann et al. (2004) suggested that the relative differences in ozone mixing ratio for different isoprene oxidation schemes can be up to 30–60%.

The modeling results here do not suggest a strong impact of biogenic emission changes on surface ozone during winter. The impact is small due to the fact that biogenic emissions are low in winter months. The small increase of BE over the Balkan Peninsula in the ECHAM run (Fig. 10) is probably due to the temperature increase as indicated also by the higher positive correlation between Δ(BE) and Δ(T) (0.51). Biogenic emissions are lower for the ECHAM run during summer, due to the mostly negative Δ(SR) and Δ(T) fields. Correlation of Δ(BE) with Δ(SR) and Δ(T) are 0.43 and 0.65, respectively (Tables 1a and 1b). A similar parameterization of biogenic emissions calculated on-line with MM5 presented in Poupkou et al. (2009) also shows that

ACPD
9, 10675–10710, 2009

the later are mostly temperature- rather than radiation dependent for summer months. Temperature increases in the southern east and west corners of the domain lead to higher biogenic emissions in ECHAM. The correlation of Δ(BE) and $\Delta(O_3)$ fields during summer is higher (0.46) implying a stronger dependence of ozone on emissions of biogenic origin during warm months.

3.6 Multiple linear regression analysis

In order to further analyze and quantify the relation between the differences in meteorological parameters and ozone concentration a step multiple linear regression method was employed. As already mentioned, the Pearson correlation coefficients R were calculated between $\Delta(O_3)$ and Δ(var), where "var" the selected meteorological parameters (Table 1). The next step was to build a simple regression model which predicts $\Delta(O_3)$ based on the behavior of Δ(var).

Using multiple regression analysis, $\Delta(O_3)$ is treated as a dependant (predictant) variable and all other parameters (Δ(GH), Δ(T), Δ(T850), Δ(SR), Δ(U), Δ(V), Δ(BE), $\Delta(NO_x)$) as independent (predictor) variables. An effort was made in order to establish a set of independent variables that gives rise to the best prediction of $\Delta(O_3)$. The number of data points (cases) used in the analysis was 9200 (100 rows×92 columns). Stepwise multiple linear regression was used to reveal the meteorological parameters related to ozone concentration. Forward stepwise regression adds or deletes the independent variables from the model at each step of the regression until the "best" regression model is obtained. Standardized regression coefficients (beta) were taken into account. The beta value is a measure of how strongly each predictor variable influences the predicted variable. The beta is measured in units of standard deviation. The higher the beta value the greater the impact of the predictor on the predicted variable.

For the goodness of fit the adjusted R-square was used. R is a measure of the correlation between each predictor and the criterion variable. R-square is the square of this measure of correlation and indicates the proportion of the variance in the predicted variable that is accounted for the statistical model. This is essentially a measure of

ACPD
9, 10675–10710, 2009

how good is the prediction of the dependent variable knowing the predictor variables. However, *R*-square tends to somewhat over-estimate the success of the model, so an Adjusted *R*-square value is calculated which takes into account the number of variables in the model and the number of cases the model is based on. This Adjusted *R*-square value gives the most useful measure of the success of the statistical model. If for example the Adjusted *R*-square value is 0.75 it means that the statistical model has accounted for 75% of the variance in the predicted variable.

Adjusted *R*-square is presented at the bottom of Tables 2a and 2b, for winter and summer, respectively, together with the statistical significance of the results. The first column of each table shows the R-square change for every variable, which is a measure of how the power of the regression model changes with the addition or removal of a predictor variable. The second column shows the beta value for each variable examined and the third its statistical significance.

Table 2a shows that almost 60% of $\Delta(O_3)$ variance can be explained for wintertime when taking into account seven out of eight variables examined. Differences of NO_x between ECHAM and ERA runs seem to explain the greatest part of O_3 changes in the regression model. Specifically, $\Delta(NO_x)$ explains ~40% of $\Delta(O_3)$ in winter. A beta value of −0.6 indicates that a change of one standard deviation in $\Delta(NO_x)$ will result in a change of 0.6 standard deviation in $\Delta(O_3)$. Almost 70% of variability in ozone can be explained during summer based on eight key meteorological parameters and NO_x. Solar radiation affects decisively ozone changes together with NOx concentrations. Together, they explain almost 50% of $\Delta(O_3)$ variance according to the statistical analysis. Among these two variables, Δ(SR) explains ~33% of $\Delta(O_3)$ in summer while $\Delta(NO_x)$ explains ~15% .

Figure 11 illustrates the predicted $\Delta(O_3)$ values as calculated by the simple regression model. Comparison of Figs. 3 and 11 shows that the change of meteorological parameters together with two important ozone precursors, NO_x and biogenic emissions, can explain the basic features of O_3 change both in absolute magnitude and its spatial pattern. The regression model describes more successfully $\Delta(O_3)$ in sum-

ACPD
9, 10675–10710, 2009

mer and slightly exaggerates on the importance of $\Delta(NO_x)$ on $\Delta(O_3)$. This is seen in Fig. 11 during summer over the English Channel, where calculation of the regression model reveals $\Delta(O_3)>0$ over the English Channel while ECHAM-ERA CAMx runs yield $\Delta(O_3)\sim0$ (Fig. 3). Such differences are also accounted during winter over the Mediterranean, the Adriatic Sea and the Iberian Peninsula. Changes in ozone are mostly affected by $\Delta(NO_x)$ according to the regression statistical model and thus O_3 increases over the Iberian Peninsula and along the Mediterranean (the impact of ship emissions is clear) while decreases over the Adriatic Sea. $\Delta(O_3)$ simulated by CAMx on the other hand, increases only in eastern Mediterranean, remains unchanged over the Adriatic Sea and very slightly decreases over the Iberian Peninsula.

4 Conclusions

In the current work a modeling system based on the air quality model CAMx driven off-line by the regional climate model RegCM3 was used for the assessment of regional air quality over Europe for the decade 1991–2000. For the external meteorological forcing two different datasets were used: the ERA40 global atmospheric reanalysis dataset and the model output from the GCM ECHAM (ERA and ECHAM runs, respectively). The focus of this work was to compare the perfect lateral boundary conditions experiment with the GCM driven control experiment and to investigate how this external meteorological forcing affects near surface ozone.

Different RegCM forcing results in $\Delta(O_3)$ ranging between ±5 ppb, while all model parameterizations and anthropogenic emissions remain unchanged. The area showing the greatest sensitivity in O_3 during winter is central and Southern Europe while in summer north and central continental Europe. Changes in ozone are induced by changes in meteorological fields and biogenic emissions, which are on-line calculated and meteorology-dependent. As indicated by the 500 hPa GH, used here as an index of atmospheric circulation, the ECHAM run reveals a more steep GH gradient along the west-east axis of Europe with lower GH over the west Atlantic and UK (more cyclonic

ACPD
9, 10675–10710, 2009

conditions) and higher GH over Eastern Europe (more anticyclonic conditions) during winter and lower GH over Russia (more cyclonic conditions) during summer. The differences in both zonal and meridional wind fields are associated with the differences in the circulation patterns. Furthermore the differences in near surface air temperature and incoming solar radiation can be partly explained by the differences in atmospheric circulation. Solar radiation appears to be the parameter mostly controlling the ozone concentrations during summer. Interestingly, the range of changes in the above mentioned meteorological parameters due to external meteorological forcing is comparable to those predicted for future climate change scenarios. The meteorology-depended biogenic emissions appear to be mostly temperature than radiation dependent. The impact of the changes in biogenic VOCs is mostly clear during summer when biogenic emissions are higher. The model simulations indicate, however, that ozone production is mainly NO_x limited. Using multiple regression analysis to associate the changes in near surface ozone with the respective changes in selected meteorological parameters and ozone precursors, an explained variance of 70% in summer and 60% in winter is reproduced. Among the predictors, Δ(SR) dominates in summer explaining ~33% of $\Delta(O_3)$ while $\Delta(NO_x)$ dominates in winter explaining ~40% of $\Delta(O_3)$.

Acknowledgements. This work has been funded by the European Community's Sixth Framework Programme as part of the project CECILIA (Central and Eastern Europe Climate Change Impact and Vulnerability Assessment) under Contract No. 037005.

References

Baertsch-Ritter, N., Keller, J., Dommen, J., and Prevot, A. S. H.: Effects of various meteorological conditions and spatial emissionresolutions on the ozone concentration and ROG/NOx limitationin the Milan area (I), Atmos. Chem. Phys., 4, 423–438, 2004, http://www.atmos-chem-phys.net/4/423/2004/.

Bloomfield, P., Royle, J. A., Steinberg, L. J., and Yang, Q.: Accounting for meteorological effects in measuring urban ozone levels and trends, Atmos. Environ., 30(17), 3067–3077, 1996.

Broennimann, S. and Neu, U.: Weekend-weekday differences of near-surface ozone concentrations in Switzerland for different meteorological conditions, Atmos. Environ., 31(8), 1127–1135, 1997.

Crutzen, P. J.: Tropospheric ozone: An overview, in: Tropospheric Ozone, edited by: Isaksen, I. S. A., D. Reidel Publ. Co., Dordrecht, The Netherlands, 3–32, 1988.

Davies, T. D., Kelly, P. M., Low, P. S., and Pierce, C. E.: Surface ozone concentrations in Europe: links with regional-scale atmospheric circulation, J. Geophys. Res., 97(D9), 9819–9832, 1992.

Davis, J. M., Eder, B. K., Nychka, D., and Yang, Q.: Modeling the effects of meteorology on ozone in Houston using cluster analysis and generalized additive models, Atmos. Environ., 32(14/15), 2505–2520, 1998.

Dawson, J. P., Adams, P. J., and Pandis, S. N.: Sensitivity of ozone to summertime climate in the eastern USA: A modeling case study, Atmos. Environ., 41, 1494–1511, 2007.

Dickinson, R., Henderson-Sellers, A., and Kennedy, P. J.: Biosphere-Atmosphere Transfer Scheme, BATS: version1E as coupled to the NCAR Community Climate Model, NCAR Technical Note No NCAR/TN-387+STR, Boulder, CO, available from the National Center for Atmospheric Research, P.O. Box 3000, Boulder, CO 80307, 72 pp., 1993.

Fiore, A. M., Horowitz, L. W., Purves, D. W., Levy, H., Evans M. J., Wang, Y., Li, Q., and Yantosca, R. M.: Evaluating the contribution of changes in isoprene emissions to surface ozone trends over the eastern United States, J. Geophys. Res., 110, D12303, doi:10.1029/2004JD005485, 2005.

Fritsch, J. M. and Chappell, C. F.: Numerical prediction of convectively driven mesoscale pressure systems. part i: Convective parameterization, J. Atmos. Sci., 37, 1722–1733, 1980.

Fuhrer, J. and Booker, F.: Ecological issues related to ozone: agricultural issues. Environ. Int., 29(2–3), 141–154, 2003.

Giorgi, F., Pal, J. S., Bi, X., Sloan, L., Elguindi, N., and Solmon, F.: Introduction to the TAC special issue: The RegCNET network, Theor. Appl. Climatol., 86, 1–4, doi:10.1007/s00704-005-0199-z, 2006.

Grell, G. A.: Prognostic evaluation of assumptions used by cumulus parametrizations, Mon. Weather Rev., 121, 764–787, 1993.

Grell, G. A., Dudhia, J., and Stauer, D. R.: A description of the fifth-generation penn state/ncar mesoscale model (mm5), Technical report NCAR/TN-398+STR, National Center for Atmospheric Research, Boulder, CO, 1994.

Guenther, A. B., Zimmermann, P. C., Harley, R., Monson, R. K., and Fall, R.: Isoprene and monoterpene emission rate variability: model evaluations and sensitivity analyses, J. Geophys. Res., 98, 12609–12617, 1993.

Hauglustaine, D. A., Lathiere, J., Szopa, S., and Folberth, G. A.: Future tropospheric ozone simulated with a climate-chemistry biosphere model, Geophys. Res. Lett., 32, L24807, doi:10.1029/2005GL024031, 2005.

Hedegaard, G. B., Brandt, J., Christensen, J. H., Frohn, L. M., Geels, C., Hansen, K. M., and Stendel, M.: Impacts of climate change on air pollution levels in the Northern Hemisphere with special focus on Europe and the Arctic, Atmos. Chem. Phys., 8, 3337–3367, 2008, http://www.atmos-chem-phys.net/8/3337/2008/.

Hegarty, J., Mao, H., and Talbot, R.: Synoptic controls on summertime surface ozone in the northeastern United States, J. Geophys. Res., 112, D14306, doi:10.1029/2006JD008170, 2007.

Intergovernmental Panel on Climate Change (IPCC): Climate Change 2007: The Physical Science Basis, 996 pp., Cambridge Univ. Press, New York, 2007.

Kalabokas, P. D., Mihalopoulos, N., Ellul, R., Kleanthous, S., and Repapis, C. C.: An investigation of the meteorological and photochemical factors influencing the background rural and marine surface ozone levels in the Central and Eastern Mediterranean, Atmos. Environ., 42, 7894–7906, doi:10.1016/j.atmosenv.2008.07.009, 2008.

Khalid, I. A.-W. and Samson, P. J.: Preliminary sensitivity analysis of Urban Airshed Model simulations to temporal and spatial availability of boundary layer wind measurements, Atmos. Environ., 30(12), 2027–2042, 1996.

Kiehl, J. T., Hack, J., Bonan, G., Boville, B., Briegleb, B., Williamson, D., and Rasch, P.: Description of the NCAR Community Climate Model (CCM3), Technical Report NCAR/TN-420+STR, National Center for Atmospheric Research, Boulder, Colorado, 152 pp., 1996.

Krüger, B. C., Katragkou, E., Tegoulias, I., Zanis, P., Melas, D., Coppola, E., Rauscher, S., Huszar, P., and Halenka, T.: Regional photochemical model calculations for Europe concerning ozone levels in a changing climate, Q. J. Hung. Meteorol. Serv., 112(3–4), 285–300, 2008.

Meleux, F., Solmon, F., and Giorgi, F.: Increase in summer European ozone amounts due to climate change, Atmos. Environ., 41(35), 7577–7587, 2007.

Nolte C. G., Gilliland, A. B., Hogrefe, C., and Mickley, L. J.: Linking global to regional models to assess future climate impacts on surface ozone levels in the United States, J. Geophys.

Res., 113, D14307, doi:10.1029/2007JD008497, 2008.
O'Brien, J. J.: A Note on the Vertical Structure of the Eddy Exchange Coefficient in the Planetary Boundary Layer. J. Atmos. Sci., 27, 1213–1215, 1970.
Pal, J. S., Small, E. E., and Eltahir, E. A. B.: Simulation of regional-scale water and energy budgets:Representation of subgrid cloud and precipitation processes within RegCM, J. Geophys. Res., 105(D24), 29579–29594, 2000.
Pal, J. S., Giorgi, F., Bi, X., Elguindi, N., Solomon, F., Gao, X., Rauscher, S. A., Francisco, R., Zakey, A., Winter, J., Ashfaq, M., Syed, F. S., Bell, J. L., Diffenbaugh, N. S., Karmacharya, J., Konare, A., Martinez, D., da Rocha, R. P., Sloan, L. C., and Steiner, A. L.: Regional climate modeling for the developing world: The ICTP RegCM3 and RegCNET, B. Am. Meteor. Soc., 88, 1395–1409, 2007.
Penkett, S. A.: Indications and causes of ozone increase in the troposphere, in: The changing atmosphere, edited by: Rowland, F. S. and Isaksen, I. S. A., J. Wiley & Sons, New York, pp. 91, 1988.
Poupkou, A., Giannaros, T., Kioutsioukis, I., Markakis, K., Melas, D., and Zerefos, C.: A biogenic NMVOCs emission model, Proceedings of the 7th International Conference on Air Quality – Science and Application, Istanbul, 24–27 March 2009.
Racherla, P. N. and Adams, P. J.: Sensitivity of global tropospheric ozone and fine particulate matter concentrations to climate change, J. Geophys. Res., 111, D24103, doi:10.1029/2005JD006939, 2006.
Racherla, P. N. and Adams, P. J.: The response of surface ozone to climate change over the Eastern United States, Atmos. Chem. Phys., 8, 871–885, 2008, http://www.atmos-chem-phys.net/8/871/2008/.
Scebba, F., Giuntini, D., Castagna, A., Soldatini, G., and Ranieri, A.: Analysing the impact of ozone on biochemical and physiological variables in plant species belonging to natural ecosystems, Env. Exp. Bot., 57, 89–97, 2006.
Schlink, U., Herbarth, O., Richter, M., Dorling, S., Nunnari, G., Cawley, G., and Pelikan, E.: Statistical models to assess the health effects and to forecast ground-level ozone, Environ. Modell. Softw., 21(4), 547–558, 2006.
Seinfeld, J. H. and Pandis, S. N.: Atmospheric Chemistry and Physics, 3rd edn., John Wiley, USA, 1998.
Sillman, S. and Samson, P. J.: Impact of temperature on oxidant photochemistry in urban, polluted rural and remote environments, J. Geophys. Res., 100(D6), 11497–11508, 1995.

Stevenson, D. S., Dentener, F. J., Schultz, M. G., Ellingsen, K., van Noije, T. P. C, Wild, O., Zeng, G., Amann, M., Atherton, C. S., Bell, N., Bergmann, D. J., Bey, I., Butler, T., Cofala, J., Collins, W. J., Derwent, R. G., Doherty, R. M., Drevet, J., Eskes, H. J., Fiore, A. M., Gauss, M., Hauglustaine, D. A., Horowitz, L. W., Isaksen, I. S. A., Krol, M. C., Lamarque, J.-F., Lawrence, M. G., Montanaro, V., Müller, J.-F., Pitari, G., Prather, M. J., Pyle, J. A., Rast, S., Rodriquez, J. M., Sanderson, M. G., Savage, N. H., Shindell, D. T., Strahan, S. E., Sudo, K., and Szopa, S.: Multimodel ensemble simulations of present-day and near-future tropospheric ozone, J. Geophys. Res., 111, D08301, doi:10.1029/2005JD006338, 2006.

Szopa, S., Hauglustaine, D. A., Vautard, R., and Menut, L.: Future global tropospheric ozone changes and impact on European air quality, Geophys. Res. Lett., 33, L18805, doi:10.1029/2006GL25860, 2006.

Tegoulias, I., Zanis, P., Katragkou, E., and Melas, D.: Validation of a long-term regional air quality simulation for Europe over the period 1991–2000 using the modelling system RegCM3/CAMx, in preparation, 2009.

Vestreng, V., Breivik, K., Adams, M., Wagener, A., Goodwin, J., Rozovskaya, O., and Pacyna, J. M.: Inventory Review 2005, Emission Data reported to LRTAP Convention and NEC Directive, Initial review of HMs and POPs, Technical report MSC-W 1/2005, ISSN 0804-2446, available at http://www.emep.int/mscw/mscw_publications.html#2005, 2005.

von Kuhlmann, R., Lawrence, M. G., Pöschl, U., and Crutzen, P. J.: Sensitivities in global scale modeling of isoprene, Atmos. Chem. Phys., 4, 1–17, 2004, http://www.atmos-chem-phys.net/4/1/2004/.

Winiwarter, W. and Zueger, J.: Pannonisches Ozonprojekt, Teilprojekt Emissionen, Endbericht, Report OEFZS-A-3817. Austrian Research Center, Seibersdorf, 1996.

Zeng, X., Zhao, M., and Dickinson, R. E.: Intercomparison of bulk aerodynamic algorithms for the computation of sea surface fluxes using toga coare and tao data, J. Climate, 11, 2628–2644, 1998.

Table 1a. Correlation between differences in selected variables during winter. All correlations are significant at $p<0.05$ with the exception of those marked with the asterisk (*).

WINTER	$\Delta(O_3)$	Δ(BE)	Δ(CLWP)	Δ(GH)	Δ(SR)	Δ(T850)	Δ(T)	$\Delta(NO_x)$	Δ(U)	Δ(V)
$\Delta(O_3)$	1.00	0.29	−0.09	0.29	0.16	0.22	0.26	−0.63	0.25	−0.08
Δ(BE)	0.29	1.00	−0.03	0.34	0.09	0.30	0.51	−0.24	0.18	0.18
Δ(CLWP)	−0.09	−0.03	1.00	−0.56	−0.66	−0.59	−0.01*	0.04	0.43	0.09
Δ(GH)	0.29	0.34	−0.56	1.00	0.41	0.95	0.46	−0.14	−0.13	−0.03
Δ(SR)	0.16	0.09	−0.66	0.41	1.00	0.50	0.15	0.00	−0.36	0.04
Δ(T850)	0.22	0.30	−0.59	0.95	0.50	1.00	0.41	−0.11	−0.22	0.01*
Δ(T)	0.26	0.51	−0.01*	0.46	0.15	0.41	1.00	−0.28	−0.05	0.06
$\Delta(NO_x)$	−0.63	−0.24	0.04	−0.14	0.00*	−0.11	−0.28	1.00	−0.06	−0.12
Δ(U)	0.25	0.18	0.43	−0.13	−0.36	−0.22	−0.05	−0.06	1.00	0.19
Δ(V)	−0.08	0.18	0.09	−0.03	0.04	0.01*	0.06	−0.12	0.19	1.00

O_3=Ozone
BE=Biogenic Emissions
CLWP=Cloud Liquid Water Path
GH=500 hPa Geopotential Height
SR=Incoming Solar Radiation
T850=850 hPa Temperature
T=surface Temperature
NO_x=Nitrogen Oxides
U=Zonal wind component
V=Meridional wind component

ACPD
9, 10675–10710, 2009

Table 1b. Correlation between differences in selected variables during summer. All correlations are significant at $p<0.05$ with the exception of those marked with the asterisk (*).

SUMMER	$\Delta(O_3)$	Δ(BE)	Δ(CLWP)	Δ(GH)	Δ(SR)	Δ(T850)	Δ(T)	$\Delta(NO_x)$	Δ(U)	Δ(V)
$\Delta(O_3)$	1.00	0.46	−0.55	0.57	0.58	0.55	0.36	−0.48	−0.24	0.36
Δ(BE)	0.46	1.00	−0.39	0.69	0.43	0.62	0.65	−0.19	−0.20	−0.01*
Δ(CLWP)	−0.55	−0.39	1.00	−0.39	−0.73	−0.32	−0.21	0.17	0.19	−0.05
Δ(GH)	0.57	0.69	−0.39	1.00	0.46	0.95	0.70	−0.21	−0.22	0.19
Δ(SR)	0.58	0.43	−0.73	0.46	1.00	0.41	0.31	−0.17	−0.22	0.10
Δ(T850)	0.55	0.62	−0.32	0.95	0.41	1.00	0.67	−0.18	−0.25	0.15
Δ(T)	0.36	0.65	−0.21	0.70	0.31	0.67	1.00	−0.26	−0.52	−0.18
$\Delta(NO_x)$	−0.48	−0.19	0.17	−0.21	−0.17	−0.18	−0.26	1.00	0.15	−0.06
Δ(U)	−0.24	−0.20	0.19	−0.22	−0.22	−0.25	−0.52	0.15	1.00	0.43
Δ(V)	0.36	−0.01*	−0.05	0.19	0.10	0.15	−0.18	−0.06	0.43	1.00

O_3=Ozone
BE=Biogenic Emissions
CLWP=Cloud Liquid Water Path
GH=500 hPa Geopotential Height
SR=Incoming Solar Radiation
T850=850 hPa Temperature
T=surface Temperature
NO_x=Nitrogen Oxides
U=Zonal wind component
V=Meridional wind component

ACPD
9, 10675–10710, 2009

Table 2a. Multiple regression analysis results for the winter period.

Δ(var)	*R*-square change	Beta	*p*
NO_x	0.399	−0.601	0.0000
Solrad	0.064	0.274	0.0000
V	0.051	−0.216	0.0000
U	0.045	0.323	0.0000
Geop	0.017	0.447	0.0000
temp850	0.009	−0.353	0.0000
biogen	0.002	0.053	0.0000

Adjusted *R*-square 0.587
$P<0$

Table 2b. Multiple regression analysis results for the summer period.

Δ(var)	*R*-square change	Beta	*p*
Solrad	0.333	0.297	0.0000
NO_x	0.152	−0.339	0.0000
temp850	0.088	0.301	0.0000
V	0.069	0.376	0.0000
U	0.033	−0.285	0.0000
biogen	0.008	0.194	0.0000
temp	0.012	−0.183	0.0000
Geop	0.000	−0.061	0.0039

Adjusted *R*-square 0.694
$P<0$

ACPD
9, 10675–10710, 2009

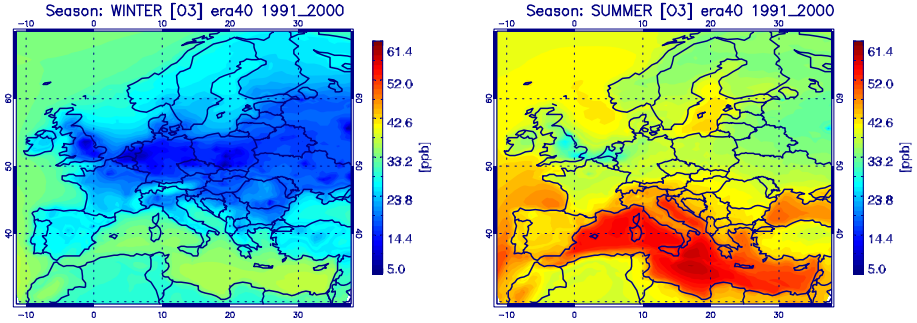

Fig. 1. Simulated average surface O_3 fields of the ERA run for winter (left) and summer (right) representative of the 1990s.

ACPD
9, 10675–10710, 2009

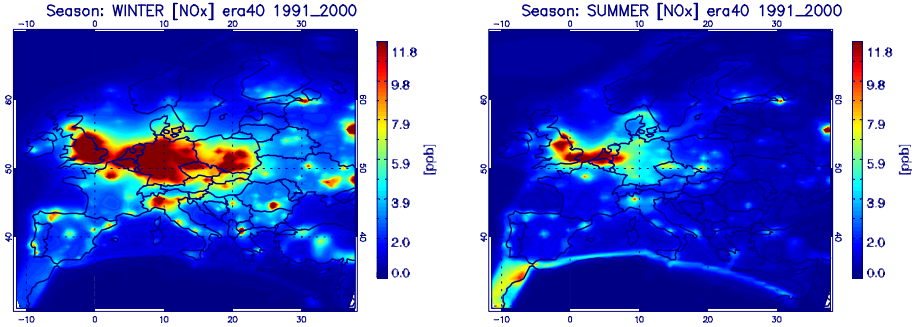

Fig. 2. Simulated average surface NO_x fields of the ERA run for winter (left) and summer (right) representative of the 1990s.

ACPD

9, 10675–10710, 2009

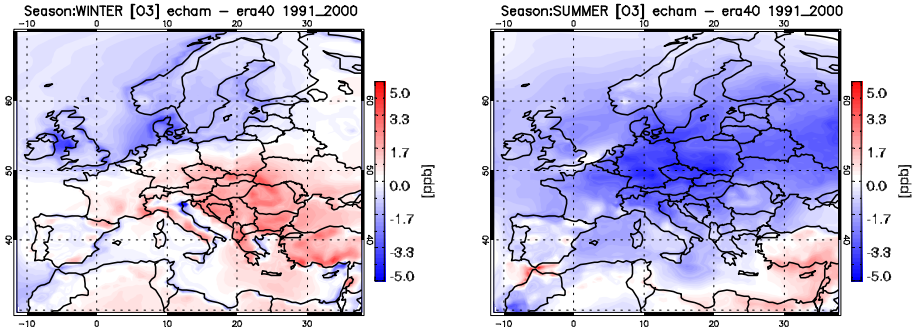

Fig. 3. Differences in simulated average O_3 fields between the ECHAM and ERA for winter (left) and summer (right) representative of the 1990s.

ACPD
9, 10675–10710, 2009

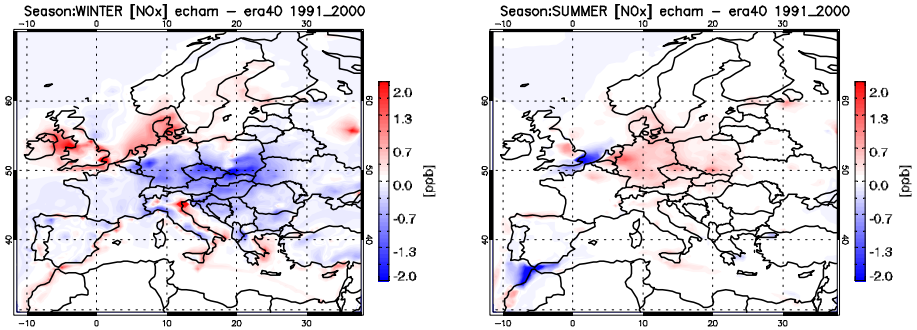

Fig. 4. Differences in simulated average NO_x fields between the ECHAM and ERA for winter (left) and summer (right) representative of the 1990s.

ACPD
9, 10675–10710, 2009

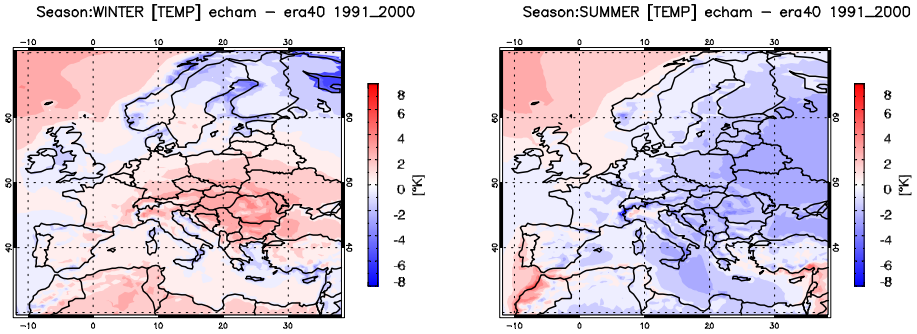

Fig. 5. Differences in simulated average temperature fields between the ECHAM and ERA for winter (left) and summer (right) representative of the 1990s.

ACPD
9, 10675–10710, 2009

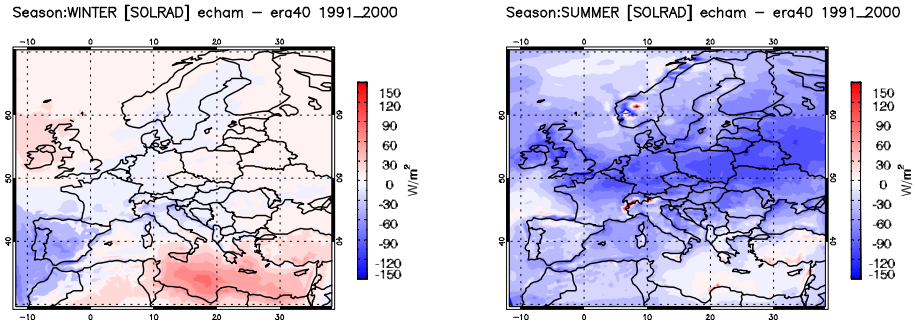

Fig. 6. Differences in simulated average solar radiation fields between the ECHAM and ERA for winter (left) and summer (right) representative of the 1990s.

ACPD
9, 10675–10710, 2009

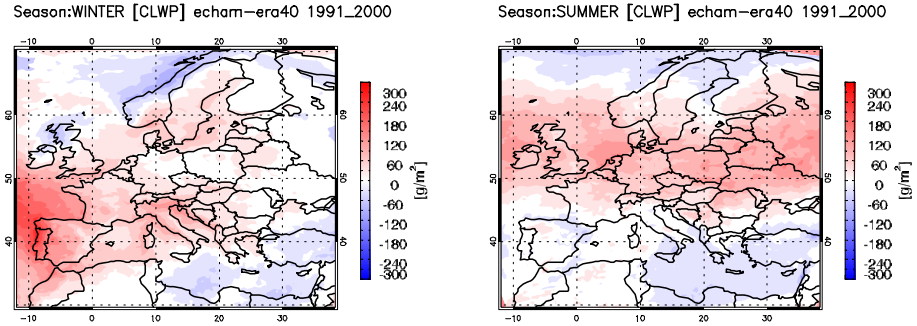

Fig. 7. Differences in simulated average cloud liquid water path fields between the ECHAM and ERA for winter (left) and summer (right) representative of the 1990s.

ACPD
9, 10675–10710, 2009

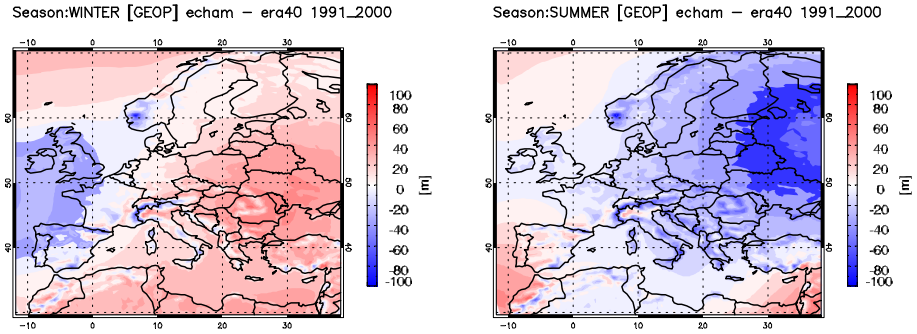

Fig. 8. Differences in simulated average 500 hPa geopotential height fields between the ECHAM and ERA for winter (left) and summer (right) representative of the 1990s.

ACPD
9, 10675–10710, 2009

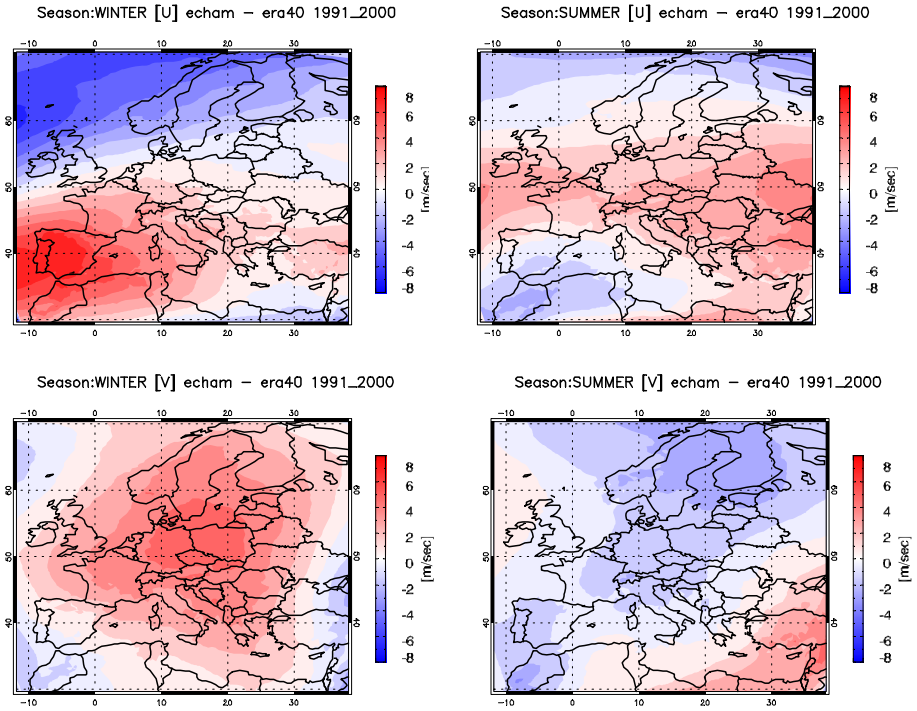

Fig. 9. Differences in simulated average meridional (U upper panel) and zonal (V bottom panel) wind component fields between the ECHAM and ERA for winter (left) and summer (right) representative of the 1990s.

ACPD
9, 10675–10710, 2009

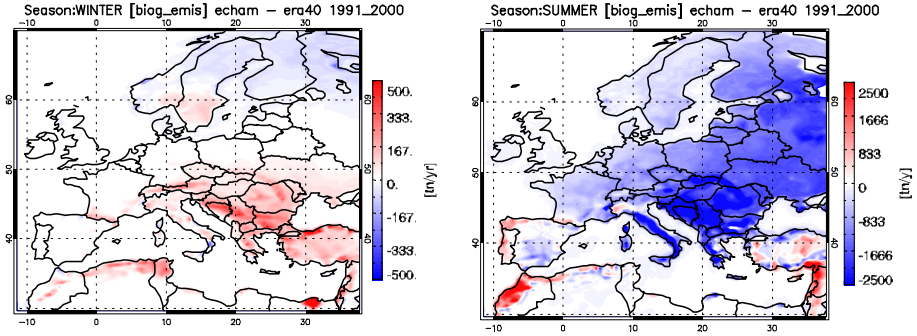

Fig. 10. Differences in simulated average biogenic emissions between the ECHAM and ERA for winter (left) and summer (right) representative of the 1990s. Mind the differences in color scales for the two seasons.

ACPD
9, 10675–10710, 2009

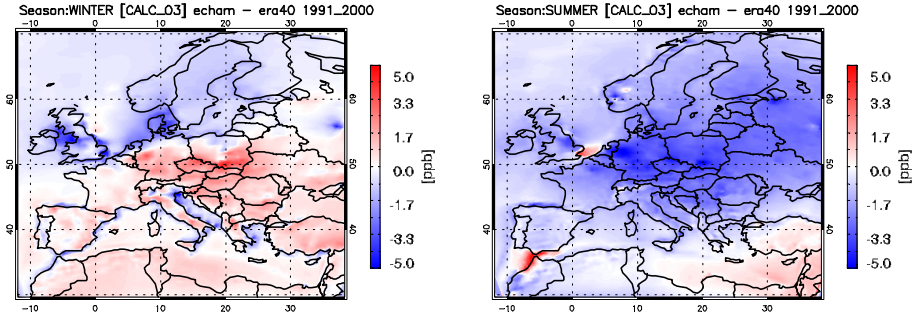

Fig. 11. Average surface O_3 fields calculated from the regression model for winter (left) and summer (right).

ACPD
9, 10675–10710, 2009